

Evaluation of Combined Contrast Agent using N-(p-maleimidophenyl) Isocyanate Linker-mediated Synthesis for Simultaneous PET-MRI

Gil-Jae Lee¹, Hwun-Jae Lee^{2,3}, Tae-Soo Lee^{4,*}

¹Department of Biomedical Engineering, Graduate School of Chungbuk National University

²Department of Radiology, College of Medicine, Yonsei University

³YUHS-KRIBB Medical Convergence Research Institute, Yonsei University

⁴Department of Biomedical Engineering, Graduate School of Chungbuk National University

Received: February 22, 2022. Revised: April 15, 2022. Accepted: April 30, 2022.

ABSTRACT

In this paper, a combined ¹⁸F-FDG (fluorodeoxyglucose) and MNP (magnetic nanoparticles) contrast agent was synthesized using N-(p-maleimidophenyl) isocyanate as the crosslinker for use in simultaneous PET-MRI scans. PET-MRI images were acquired and evaluated before and after injection of the combined contrast imaging agent (¹⁸F-FDG labeled MNP) from a glioma stem cell mouse model. After setting the region of interest (ROI) on each acquired image, the area of the lesion was calculated by segmentation. As a result, the PET image was larger than the MRI. In particular, the simultaneous PET-MRI images showed accurate lesions along with the surrounding soft tissue. The mean and standard deviation values were higher in the MRI images alone than in the PET images or the simultaneous PET-MRI images, regardless of whether the contrast agent was injected. In addition, the simultaneous PET-MRI image values were higher than for the PET images. For PSNR experiments, the original image was PET Image using ¹⁸F-FDG, MRI using MNPs, and MRI without contrast medium, and the target image was simultaneous PET-MRI image using ¹⁸F-FDG labeled MNPs contrast medium. As a result, all of them appeared significantly, suggesting that the ¹⁸F-FDG labeled MNPs contrast medium is useful. Future research is needed to develop an agent that can simultaneously diagnose and treat through SPECT-MRI imaging research that can use various nuclides.

Keywords: Simultaneous PET-MRI, Imaging agents, Evaluation contrast effect, Image processing, PSNR, Magnetic resonance imaging

I. INTRODUCTION

Combining a single device to simultaneously acquire two data sets from Positron Emission Tomography (PET) and Magnetic Resonance Imaging (MRI) scans has been of interest in research and clinical applications since before the advent of combined Positron Emission Tomography-Computed Tomography (PET-CT) devices^[1], which can be combined due to the complementary nature of the information provided by the two

powerful imaging techniques. PET uses radionuclides that decay by positron emission and is used to analyze a wide range of biological processes with very high molecular sensitivity. However, PET lacks the spatial resolution to provide the anatomical detail needed for clinical interpretation^[2]. On the other hand, MRI provides high-resolution anatomical images with excellent soft tissue contrast, even if used in a typical pulse sequence. More advanced MRI sequences allow the study of water diffusion, blood oxygen concentration-

* Corresponding Author: Tae-Soo Lee

E-mail: tslee@chungbuk.ac.kr

Tel: +82-43-261-3172

dependent contrast, and relative concentrations of various metabolites, and contrast can be further enhanced with the addition of gadolinium and iron oxide^[3]. Although Positron Emission Tomography-Magnetic Resonance Imaging(PET-MRI) scan data can be fused, fusion methods can cause erroneous scan values because the scan values fluctuate with time. Simultaneous Positron Emission Tomography- Magnetic Resonance Imaging (Simultaneous PET-MRI) scans do not cause errors in data according to scan time, and spatial registration between two images, workflow, and comfort can be improved for patients who need to undergo both examinations^[4,5]. In this paper, we examined images that were acquired using a combined contrast agent using the N-(p-maleimidophenyl) isocyanate (PMPI) crosslinker to synthesize the nuclide ¹⁸F-FDG (fluorodeoxyglucose) required for PET with the contrast agent required for MRI Magnetic Nanoparticles(MNPs) for use in simultaneous PET-MRI scans. Images before and after contrast agent injection were compared. All animal experiments were conducted with the approval of the Association for Assessment and Accreditation of Laboratory Animal Care(AAALAC) International.

II. MATERIAL AND METHODS

1. Simultaneous PET-MRI

Simultaneous PET-MRI uses radiopharmaceuticals that emit positrons and PET that can display biochemical and functional images of the human body in three dimensions and uses superconducting magnets and radio waves to protect tissues and blood vessels of the human body. It is a device that can simultaneously perform MRI, which examines humans in three dimensions^[5]. Since it is an all-in-one device, PET-MRI simultaneously acquires both images such that examination time can be reduced by nearly half compared to the sequential equipment that obtains PET and MRI images sequentially^[6]. The combination of PET and MRI is a significant technological advance in the measurement and processing of

imaging signals alongside the influence of the magnetic field by the superconducting magnet of MRI, attenuation and motion compensation, and the design error of new RF coils in the amplification device of the PET ratio^[7,8]. PET-MRI is a fusion imaging system that combines PET showing ultra-sensitive molecular imaging and MRI capable of high-resolution functional imaging^[10]. Compared to PET-CT, PET-MRI exposes the patient to less radiation, as up to 70% of the dose received from PET-CT scans is due to Computed Tomography(CT), and demonstrates higher soft tissue contrast^[9].

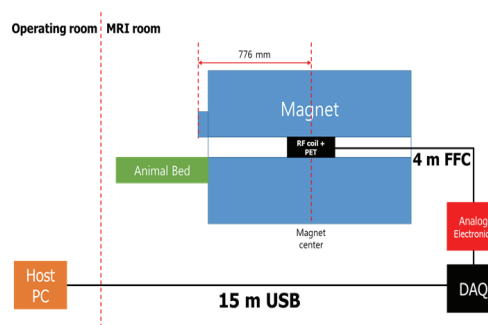


Fig. 1. Simultaneous Multiparametric PET/MRI.

2. PMPI linker-mediated PET-MRI contrast agent

Recently, medical imaging using hybrid technology has been widely accepted and used in clinical practice. Since simultaneous PET-MRI offers significant advantages over well-established PET-CT, including superior contrast and resolution and reduced ionizing radiation^[11], simultaneous PET-MRI is useful in oncological imaging of areas such as the brain, head and neck, liver, and pelvis. Nanoscale particles can exhibit special physical and biological behaviors and unique interactions with biomolecules^[12].

Nanoparticles have a large surface area and unique functions that alter pharmacokinetics, prolong vascular circulation time, improve extravasation capacity, ensure enhanced biodistribution in vivo, and induce sustained and controllable delivery^[13]. In addition,

when a specific targeting ligand is conjugated to a nanoparticle, the nanoparticle can realize its target binding ability to a diseased region^[14]. Nanocarriers penetrate through microvessels with improved permeability and are then absorbed into cells, resulting in highly selective payload accumulation at the target site^[15].

Over the past few decades, many traditional medical imaging techniques have been established for routine laboratory and clinical use. These imaging techniques, including optical imaging(OI), CT, MRI, ultrasound(US), and PET-single photon emission computed tomography(PET/SPECT) radionuclide imaging, have been widely applied in small-scale experiments and have shown excellent performance^[16]. Molecular imaging differs from conventional imaging in that it is used to image specific targets or pathways using probes known as biomarkers. Biomarkers must interact very specifically with their surrounding environment and change their image in response to molecular changes occurring within the region of interest(ROI). Molecular imaging agents are endogenous molecular or exogenous probes used to visualize, characterize, and quantify biological processes in living systems. Different imaging techniques in terms of sensitivity, resolution, and complexity often require specific contrast agents to achieve satisfactory contrast enhancement in visualization reconstructions^[16].

Here, we describe a new PET-MRI combined contrast medium. Iron oxides(IONPs) are favored for T2 and T2*-weighted MRI imaging. There are several methods for the chemical synthesis of iron oxide nanoparticles. Among these methods, coprecipitation of Fe²⁺ and Fe³⁺ ions in a basic aqueous medium (NaOH or NH₄OH solution) is the simplest, but generally polydisperse non-crystallized nanoparticles are obtained^[17]. To avoid these disadvantages, iron oxide nanoparticles that are monodisperse and of uniform crystallinity were prepared using a thermal

decomposition method. Then, the hydrophobic iron oxide nanoparticles can be coated with phospholipids, silica, or an amphiphilic polymer as a shell to exhibit excellent solubility and biocompatibility in vivo^[17]. In the simultaneous PET-MRI units, the PET is placed within the MR bore. To acquire simultaneous PET-MRI images, a combined imaging agent must be metabolized simultaneously in the body^[18]. Therefore, the MRI and PET contrast agents should be synthesized as one agent. Here, we used PMPI to crosslink MNPs for MRI imaging with ¹⁸F-FDG for PET imaging as a single contrast agent for combined PET-MRI imaging (Fig. 2).

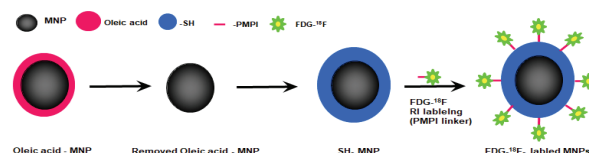


Fig. 2. ¹⁸F-FDG labeled MNPs.

In general, the MNPs are coated with oleic acid to maintain uniform dispersion. However, the coated MNPs cannot be directly injected in vivo due to toxicity. Therefore, after removing the toxicity with hexane, which is usually a strong acid, it is substituted with a biocompatible polymer biomaterial^[19]. In this study, ¹⁸F-FDG was attached to the MNPs by electrostatic attraction to the MNP surface by removing oleic acid using specific conditions and leaving an SH-group that is frequently expressed on the metal surface^[20]. The ¹⁸F-FDG and MNP attachment occurs when they are subjected to a physical reaction by centrifugation, whereby SH-MNPs with a relatively heavy molecular weight, exist on the inside by centrifugal force and the water-soluble ¹⁸F-FDG with a relatively lighter molecular weight, stays on the surface^[21]. The magnetic SH- group and the OH-group of ¹⁸F-FDG are conjugated by the PMPI crosslinker.

3. Image evaluation

Image quality evaluation characterizes the content and texture of an image. Basically, evaluation metrics can be categorized into primary, secondary, and higher order scales. Primary metrics focus on properties such as the mean intensity, standard deviation, and variance and first-order metrics only have an effect on individual pixels in the image. First-order metrics do not account for spatial relationships between pixels, and therefore do not address neighbor relationships^[22,23]. On the other hand, quadratic or higher metrics measure the properties of two or more pixels that occur relative to each other at a specific location. In medical images, the mean is often used as a matrix representative value of pixels^[24]. The standard deviation, seen in scatter plots, is a representative number indicating how spread out the medical image pixel data is around the mean^[24]. A standard deviation close to 0 means that the data values are concentrated near the mean, and a larger standard deviation means that the data values are spread out^[25].

Peak signal to noise ratio(PSNR) is the maximum signal-to-noise ratio. It is an objective measurement method that numerically indicates the difference between the image before and after contrast medium injection during medical image evaluation. PSNR is most easily defined via the mean squared error (MSE)^[25,26]. For a before contrast agent injection $m \times n$ monochrome image I , and after contrast agent injection image approximation K , MSE is defined as:

$$MSE = \frac{1}{m \cdot n} \sum_{i=0}^{m-1} \sum_{j=0}^{n-1} [I(i, j) - K(i, j)]^2 \quad (1)$$

The PSNR (in dB) is defined as:

$$\begin{aligned} PSNR &= 10 \cdot \log_{10} \left(\frac{MAX_I^2}{MSE} \right) \\ &= 20 \cdot \log_{10} \left(\frac{MAX_I}{\sqrt{MSE}} \right) \\ &= 20 \cdot \log_{10}(MAX_I) - 10 \cdot \log_{10}(MSE) \end{aligned} \quad (2)$$

Here, MAX_I is the maximum possible pixel value of the image. When the pixels are represented using an 8 bit per sample, this is 255. More generally, when samples are represented using linear pulse-code modulation (PCM) with B bits per sample, MAX_I is $2^B - 1$. Image processing for image evaluation was performed by writing an M-program using the MATLAB® Image Processing Toolbox as shown in Fig. 3.

```

imshow(1);
title('Weighted (red) and Unweighted (blue) Centroids');
hold on
numObj = numel(s);
for k = 1 : numObj
    plot(s(k).WeightedCentroid(1), s(k).WeightedCentroid(2), 'r+');
    plot(s(k).Centroid(1), s(k).Centroid(2), 'bo');
end
hold off
%-----
% Step 4: Calculate Custom Pixel Value-Based Properties
s = regionprops(BW, I, {'Centroid', 'PixelValues', 'BoundingBox'});
imshow(1); title('Standard Deviation of Regions');
hold on
for k = 1 : numObj
    s(k).StandardDeviation = std(double(s(k).PixelValues));
    text(s(k).Centroid(1), s(k).Centroid(2), ...
        sprintf('%2.1f', s(k).StandardDeviation), ...
        'EdgeColor', 'b', 'Color', 'r');
end
hold off
% label number.
%-----
figure
bar(1:numObj, [s.StandardDeviation])
xlabel('Region Label Number')
ylabel('Standard Deviation')
%-----

```

Fig. 3. Example of M-programing for image evaluation.

III. EXPERIMENT AND RESULT

The experiment was carried out as outlined in Fig. 4. After preparing the ^{18}F -FDG labeled MNPs combined contrast agent for simultaneous PET-MRI, images were acquired with a simultaneous PET-MRI device. The acquired and stored images were pre-processed with an 8-bit depth of 256 x 256 pixels for image processing, and then entered into the MATLAB® program. First, the following images were processed: pre-injection MRI images, MNP contrast agent MRI images, ^{18}F -FDG contrast agent

PET images, and ^{18}F -FDG labeled MNP contrast agent simultaneous PET-MRI images. Then, the images were used to define the ROI, followed by segmentation of the ROI. Next, the acquired images were expressed as a three-dimensional figure with a surface plot. Finally, PSNR values were obtained to evaluate the efficiency of the combined ^{18}F -FDG labeled MNP PET-MRI contrast agent.

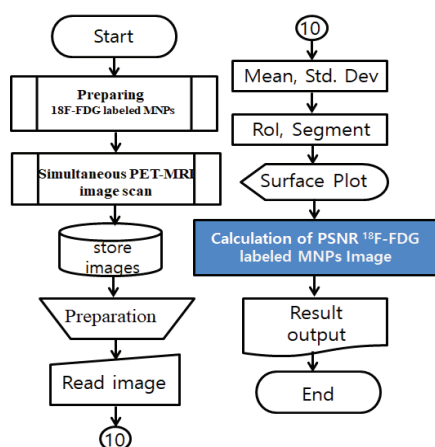


Fig. 4. Flow-chart of the experimental process.

1. Image acquisition by the simultaneous PET-MRI

For the experimental images, a coronal section was obtained four weeks after transplanting U87 glioma stem cells into a mouse model. MRI images were acquired with no contrast agent and after MNP contrast agent injection. PET images were acquired after the injection of ^{18}F -FDG contrast agent, and

finally, simultaneous PET-MRI images were acquired after injection of the ^{18}F -FDG labeled MNP contrast agent. Table 1 shows representative acquired images.

2. Processing acquired images

After preprocessing the obtained experimental images to 256 X 256 pixels and 8 bits in-depth, the mean value and standard deviation were calculated. Table 2 shows the mean value and standard deviation for each set of experimental images.

Table 2. Mean value and standard deviation of experimental images

Device	Imaging agent	Method	Value
Simultaneous PET-MRI	^{18}F -FDG labeled MNPs	Mean	32.7622
		Standard Deviation	38.8094
PET	^{18}F -FDG	Mean	16.2275
		Standard Deviation	23.1136
MRI	MNP	Mean	55.1916
		Standard Deviation	56.5563
MRI	None	Mean	59.0839
		Standard Deviation	60.5827

The ROI was set for the following acquired images: simultaneous PET-MRI (^{18}F -FDG labeled MNP contrast agent), PET (^{18}F -FDG), MRI (MNP), and MRI (no contrast agent) using the MATLAB M-program. Then, the set ROI was segmented, and a surface plot was performed. The performance results are shown in Tables 3 through 6.

Table 1. Image acquisition via the simultaneous PET-MRI device

MRI		PET	Simultaneous PET-MRI
None	MNP injection	^{18}F -FDG injection	^{18}F -FDG labeled MNP injection

Table 3. Simultaneous PET-MRI (^{18}F -FDG labeled MNP contrast agent) image processing

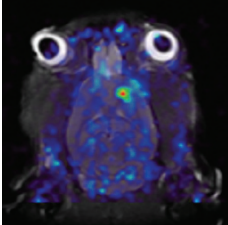
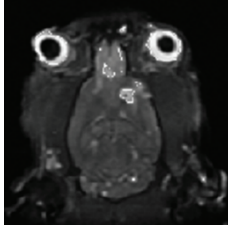
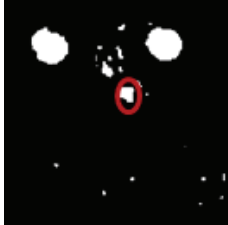
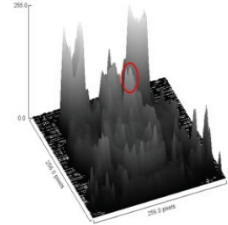
^{18}F -FDG labeled MNPs	ROI	Segmentation	Surface Plot
			

Table 4. PET (^{18}F -FDG contrast agent) image processing

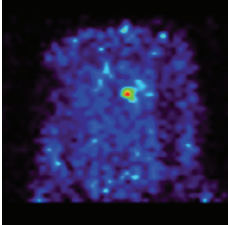
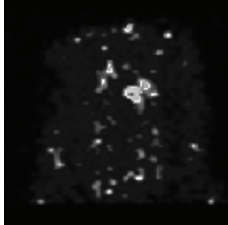

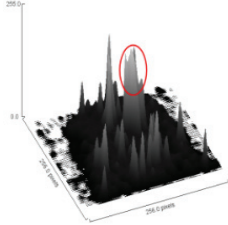
^{18}F -FDG Injection	ROI	Segmentation	Surface Plot
			

Table 5. MRI (MNP contrast agent) image processing


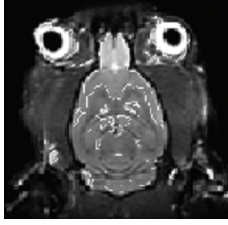

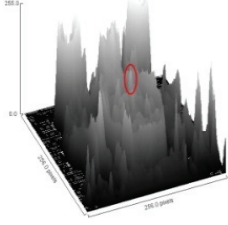
MRI MNP injection	ROI	Segmentation	Surface Plot
			

Table 6. MRI (no contrast agent) image processing

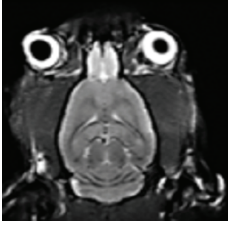
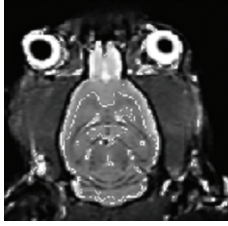

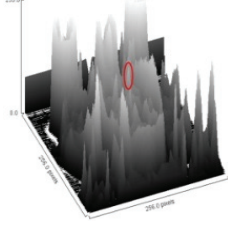
MRI Pre-injection	ROI	Segmentation	Surface Plot
			

Table 7. Results of PSNR between PET (^{18}F -FDG) and PET-MRI (^{18}F -FDG labeled MNP)

Origin image	Target image	Method	Results
PET (^{18}F -FDG)	Simultaneous PET-MRI (^{18}F -FDG labeled MNP)	MSE	1690.1609
		RMSE	41.1116
		PSNR	15.8515 dB

Table 8. Results of PSNR between MRI (MNP) and PET-MRI (^{18}F -FDG labeled MNP)

Origin image	Target image	Method	Results
MRI (MNP)	Simultaneous PET-MRI (^{18}F -FDG labeled MNP)	MSE	1871.9511
		RMSE	43.2661
		PSNR	15.4079 dB

Table 9. Results of PSNR between MRI (no contrast agent) and PET-MRI (^{18}F -FDG labeled MNP)

Origin image	Target image	Method	Results
MRI (none)	Simultaneous PET-MRI (^{18}F -FDG labeled MNP)	MSE	3254.2386
		RMSE	57.0459
		PSNR	13.0063 dB

IV. DISCUSSION

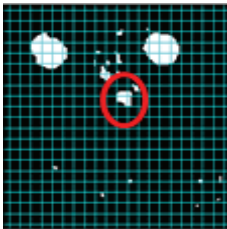
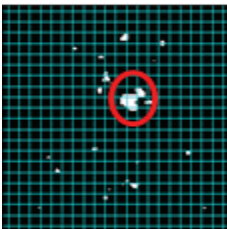
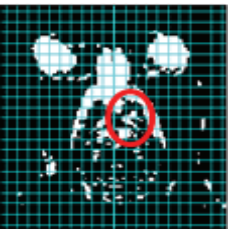
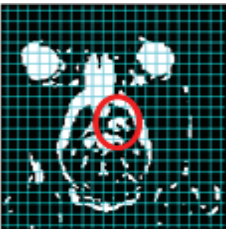
The obtained experimental images were segmented after setting the ROI and the area of the lesion was examined by attaching a grid to the segmented image. As a result, it was found that there was no significant

difference in the lesion area in the MRI image regardless of the use of MNP as the contrast agent. Simultaneous PET-MRI images using the ^{18}F -FDG labeled MNP contrast agent and PET images using the ^{18}F -FDG contrast agent showed clearer outlines of the lesion compared to MRI alone^[27]. Table 10 shows the mutual comparison of the area of the lesion by the grid, and shows that PET has better accuracy than MRI. It can be seen that the images acquired from PET show a clear distinction between surrounding tissues and lesions relative to MRI^[27,28]. In PET and simultaneous PET-MRI, the PET image shows a large lesion area, which is thought to be due to the difference between the used contrast imaging agents (^{18}F -FDG and ^{18}F -FDG labeled MNP)^[29].

Simultaneous PET-MRI imaging, similar to MRI, is capable of observing high-contrast soft tissue, which has the advantages of MRI^[30].

Fig. 5 shows the average value and standard deviation of the signal for each experimental image. The mean and standard deviation values were higher for the MRI images than both the PET or simultaneous PET-MRI images, regardless of whether contrast agents were used, and simultaneous PET-MRI images were higher than PET images. These results indicate that MRI is an imaging device with a high signal-to-noise ratio(SNR). The reason why simultaneous PET-MRI images have higher mean and standard deviation values than PET images is thought to be due to the action of MNPs.

Table 10. Area comparison of the lesion site

	Simultaneous PET-MRI	PET	MRI	
	^{18}F -FDG labeled MNP	^{18}F -FDG	MNP	None
Grid				

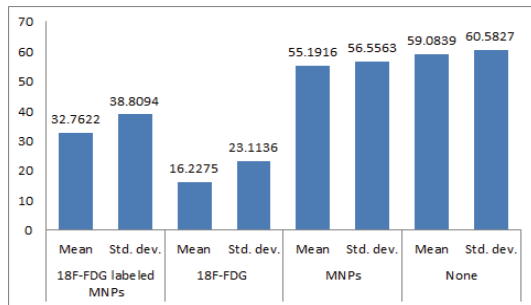


Fig. 5. Mean value and standard deviation for each pixel of experimental images.

Fig. 6 shows the PSNR as calculated below:

1) PSNR was calculated using simultaneous PET-MRI images (^{18}F -FDG labeled MNP) as the target image and PET images (^{18}F -FDG) as the original image.

2) PSNR was calculated using simultaneous PET-MRI images (^{18}F -FDG labeled MNP) as the target image and MRI images (MNPs) as the original image.

3) PSNR was calculated using simultaneous PET-MRI images (^{18}F -FDG labeled MNP) as the target image and MRI images (no contrast agent) as the original image.

As shown in Fig. 6, the PSNR obtained using the simultaneous PET-MRI image (^{18}F -FDG labeled MNP) as the target image and the PET image (^{18}F -FDG) as the original image had the highest value of 15.85 dB.

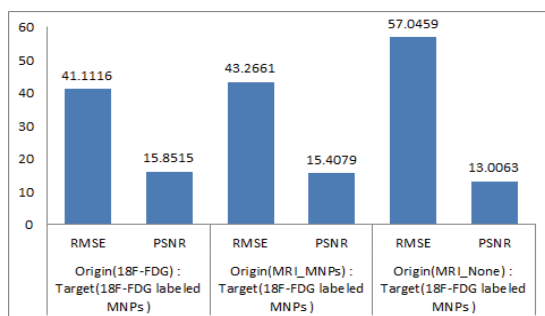


Fig. 6. PSNR values of the simultaneous PET-MRI image using the ^{18}F -FDG labeled MNP contrast agent.

V. CONCLUSION

In this paper, the enhancement effect of the ^{18}F -FDG labeled MNP simultaneous PET-MRI scan imaging contrast agent was evaluated in a glioma stem cell mouse model. For evaluation, images were acquired with the simultaneous PET-MRI ^{18}F -FDG labeled MNP contrast agent, PET images alone with ^{18}F -FDG contrast agent, MRI images alone with MNP contrast agent, and MRI images with no contrast agent were obtained for comparison.

After setting the ROI on each acquired image, the area of the lesion was calculated by segmentation. As a result, the PET image was larger and more accurate than the MRI image. In particular, the simultaneous PET-MRI image showed accurate lesions and the surrounding soft tissue. The mean and standard deviation values were higher for the MRI images than both the PET or simultaneous PET-MRI images, regardless of whether contrast agents were used, and simultaneous PET-MRI images were higher than PET images. The PSNR value showed a significant value in all experiments and showed the greatest value when the simultaneous PET-MRI image (^{18}F -FDG labeled MNP) was used as the target image and the PET image (^{18}F -FDG) was used as the original image.

In conclusion, the usefulness of the ^{18}F -FDG labeled MNP combined contrast agent as a simultaneous PET-MRI imaging agent was confirmed. Future research is required to develop an agent that can simultaneously diagnose and treat through SPECT-MRI imaging that can be used with various nuclides.

Reference

- [1] D. W. Townsend, T. Beyer, T. M. Blodgett, "PET/CT scanners: A hardware approach to image fusion", *Seminars in Nuclear Medicine*, Vol. 33, No. 3, pp. 193-204, 2003.
<http://dx.doi.org/10.1053/snuc.2003.127314>

- [2] D. W. Townsend, J. P. J. Carney, J. T. Yap, N. C. Hall, "PET/CT today and tomorrow", *Journal of Nuclear Medicine*, Vol. 45, pp. 4-14, 2004.
- [3] Y. Shao, S. R. Cherry, K. Farahani, K. Meadors, S. Siegel, R. W. Silverman, P. K. Marsden, "Simultaneous PET and MR imaging", *Physics in Medicine And Biology*, Vol. 42, No. 10, pp. 1965-1970, 1997.
<http://dx.doi.org/10.1088/0031-9155/42/10/010>
- [4] J. E. Mackewn, D. Strul, W. A. Hallett, P. Halsted, R. A. Page, S. F. Keevil, S. C. R. Williams, S. R. Cherry, P. K. Marsden, "Design and development of an MR-compatible PET scanner for imaging small animals", *IEEE transactions on nuclear science*, Vol. 52, No. 5, pp. 1379-1380, 2005.
<http://dx.doi.org/10.1109/TNS.2005.858260>
- [5] H. Zaidi, A. D. Guerra, "An outlook on future design of hybrid PET/MRI systems", *Medical Physics*, Vol. 38, No. 10, pp. 5667-5689, 2011.
<http://dx.doi.org/10.1118/1.3633909>
- [6] J. F. Valliant, "A bridge not too far: Linking disciplines through molecular imaging probes", *Journal of Nuclear Medicine*, Vol. 51, No. 8, pp. 1258-1268, 2010.
<http://dx.doi.org/10.2967/jnumed.109.068312>
- [7] R. Weissleder, M. J. Pittet, "Imaging in the era of molecular oncology", *Nature*, Vol. 452, No. 7187, pp. 580-589, 2008. <https://doi.org/10.1038/nature06917>
- [8] T. Beyer, D. W. Townsend, T. Brun, P. E. Kinahan, M. Charron, R. Roddy, J. Jerin, J. Young, L. Byars, R. Nutt, "A combined PET/CT scanner for clinical oncology", *Journal of Nuclear Medicine*, Vol. 41, No. 8, pp. 1369-1290, 2000.
- [9] B. J. Pichler, A. Kolb, T. Nagele, H. P. Schlemmer, "PET/MRI: Paving the way for the next generation of clinical multimodality imaging applications", *Journal of Nuclear Medicine*, Vol. 51, No. 3, pp. 333-336, 2010.
<http://dx.doi.org/10.2967/jnumed.109.061853>
- [10] H. Zaidi, M. L. Montandon, A. Alavi, "The clinical role of fusion imaging using PET, CT, and MR imaging", *Magnetic Resonance Imaging Clinics of North America*, Am. Vol. 18, No. 1, pp. 133-149, 2010. <https://doi.org/10.1016/j.mric.2009.09.010>
- [11] G. J. Lee, Fitting Map Analysis of Simultaneous MR-PET Images by Artificial Intelligence, Nambu University Graduate School of Radiology Master's Thesis, pp. 4-9, 2020.
- [12] R. R. Raylman, S. Majewski, S. K. Lemieux, S. S. Velan, B. Kross, V. Popov, M. F. Smith, A. G. Weisenberger, C. Zorn, G. D. Marano, "Simultaneous MRI and PET imaging of a rat brain", *Physics In Medicine And Biology*. Vol. 51, No. 24, pp. 6371-6379, 2006.
<http://dx.doi.org/10.1088/0031-9155/51/24/006>
- [13] Z. Cheng, A. A. Zaki, J. Z. Hui, V. R. Muzykantov, A. Tsourkas, "Multifunctional Nanoparticles: Cost Versus Benefit of Adding Targeting and Imaging Capabilities", *Science*, Vol. 338, No. 6109, pp. 903-910, 2012.
<http://dx.doi.org/10.1126/science.1226338>
- [14] E. F. Craparo, M. L. Bondi, G. Pitarresi, G. Cavallaro, "Nanoparticulate Systems for Drug Delivery and Targeting to the Central Nervous System", *CNS: Neuroscience and Therapeutics*, Vol. 17, No. 6, pp. 670-677, 2011.
<http://dx.doi.org/10.1111/j.1755-5949.2010.00199.x>
- [15] L. Chen, W. Hong, W. Ren, T. Xu, Z. Qian, Z. He, "Recent progress in targeted delivery vectors based on biomimetic nanoparticles", *Signal Transduction and Targeted Therapy*, Vol. 6, pp. 1-25, 2021.
<http://dx.doi.org/10.1038/s41392-021-00631-2>
- [16] L. Cunha, I. Horvath, S. Ferreira, J. Lemos, P. Costa, D. Vieira, D. S. Veres, K. Szigeti, T. Summavielle, D. Máthé, L. F. Metello, "Preclinical Imaging: an Essential Ally in Modern Biosciences", *Molecular Diagnosis & Therapy*, Vol. 18, No. 2, pp. 153-173, 2014.
<http://dx.doi.org/10.1007/s40291-013-0062-3>
- [17] M. Swierczewska, S. Lee, X. Chen, "Inorganic Nanoparticles for Multimodal Molecular Imaging", *Molecular Imaging*, Vol. 10, No. 1, pp. 3-16, 2011.
<http://dx.doi.org/10.2310/7290.2011.00001>
- [18] J. C. Patrick, Developments in PET-MRI for Radiotherapy Planning Applications, *Electronic Thesis and Dissertation Repository*. 4535, 2017. <https://ir.lib.uwo.ca/etd/4535>
- [19] A. Hervault, N. T. K. Thanh, "Magnetic

- nanoparticle-based therapeutic agents for thermo-chemotherapy treatment of cancer", *Nanoscale*, Vol. 6, No. 20, pp. 11553-11573, 2014. <http://dx.doi.org/10.1039/C4NR03482A>
- [20] Y. Hu, L. Meng, L. Niu, Q. Lu, "Highly cross-linked and biocompatible polyphosphazene-coated superparamagnetic Fe₃O₄ nanoparticles for magnetic resonance imaging", *Journal of the American Chemical Society*, Vol. 29, pp. 9156-9163, 2013. <http://dx.doi.org/10.1021/la402119s>
- [21] S. Purushotham, P. E. J. Chang, H. Rumpel, I. H. C. Kee, R. T. H. Ng, P. K. H. Chow, C. K. Tan, R. V. Ramanujan, "Thermoresponsive core-shell magnetic nanoparticles for combined modalities of cancer therapy", *Nanotechnology*, Vol. 20, No. 30, pp. 305101, 2009. <http://dx.doi.org/10.1088/0957-4484/20/30/305101>
- [22] H. Hermessi, O. Mourali, E. Zagrouba, "Multimodal medical image fusion review: Theoretical background and recent advances", *Signal Processing*, Vol. 183, pp. 108038, 2021. <https://doi.org/10.1016/j.sigpro.2021.108036>
- [23] L. Ma, W. Lin, C. Deng, K. N. Ngan, "Image retargeting quality assessment: a study of subjective scores and objective metrics", *IEEE Journal of Selected Topics in Signal Processing*, Vol. 6, No. 6, pp. 626-639, 2012. <http://dx.doi.org/10.1109/JSTSP.2012.2211996>
- [24] L. Ma, S. Li, F. Zhang, K. N. Ngan, "Reduced-reference image quality assessment using reorganized DCT-based image representation", *IEEE Transactions on Multimedia*, Vol. 13, No. 4, pp. 824-829, 2011. <http://dx.doi.org/10.1109/TMM.2011.2109701>
- [25] Mredhula. L, M. A. Dorairangaswamy, "An Extensive Review of Significant Researches on Medical Image Denoising Techniques", *International Journal of Computer Applications*, Vol. 64, No. 14, pp. 0975-8887, 2013. <http://dx.doi.org/10.5120/10699-1551>
- [26] K. S. Kang, J. H. Lee, "PSNR Appraisal of MRI Image", *Journal of the Korean Society of Radiology*, Vol. 3, No. 4, pp. 13-21, 2009.
- [27] S. C. Chan, C. H. Yeh, T. C. Yen, S. H. Ng, J. T. C. Chang, C. Y. Lin, Y. M. Tsang, K. H. Fan, B. S. Huang, C. L. Hsu, K. P. Chang, H. M. Wang, C. T. Liao, "Clinical utility of simultaneous whole-body 18F-FDG PET/MRI as a single-step imaging modality in the staging of primary nasopharyngeal carcinoma", *European Journal of Nuclear Medicine and Molecular Imaging*, Vol. 45, No. 8, pp. 1297-1308, 2018. <http://dx.doi.org/10.1007/s00259-018-3986-3>
- [28] Mohammad Reza Hayeri, Pouya Ziai, Monda L. Shehata, Oleg M Teytelboym, Brady K Huang, "Soft-Tissue Infections and Their Imaging Mimics: From Cellulitis to Necrotizing Fasciitis", *Radiographics :a review publication of the Radiological Society of North America, Inc*, Vol. 36, No. 6, pp. 1888-1910, 2016. <http://dx.doi.org/10.1148/rg.2016160068>
- [29] J. I. Kim, I. S. Kim, H. J. Lee, J. E. Kim, "Effect of MRI Media Contrast on PET/MRI", *The Korean Journal of Nuclear Medicine Technology*, Vol. 18, No. 1, pp. 19-25, 2014.
- [30] M. Hofmann, I. Bezrukov, F. Mantlik, P. Aschoff, F. Steinke, T. Beyer, B. J. Pichler, B. Schölkopf, "MRI-based attenuation correction for whole-body PET/MRI: quantitative evaluation of segmentation- and atlas-based methods", *Journal of Nuclear Medicine*, Vol. 52, No. 9, pp. 1392-1399, 2011. <http://dx.doi.org/10.2967/jnumed.110.078949>

동시 PET-MRI를 위한 N-(p-maleimidophenyl) isocyanate linker-매개 합성을 이용한 복합 조영제의 평가

이길재¹, 이훈재^{2,3}, 이태수^{4,*}

¹충북대학교 대학원 의용생체공학과

²연세대학교 의과대학 영상의학과

³연세대학교세브란스병원-한국생명공학연구소 병설 의료융합연구소

⁴충북대학교 대학원 의용생체공학과

요 약

이 논문에서는 결합된 PET(fluorodeoxyglucose, ¹⁸F-FDG)와 MRI(magnetic nanoparticles, MNP) 조영제를 동시 PET-MRI 스캔에 사용하기 위한 가교제로 N-(p-maleimidophenyl) isocyanate를 사용하여 합성하는 방안을 제안하였다. 실험은 신경교종 줄기 세포 마우스 모델에서 결합 조영제(¹⁸F-FDG로 표지된 MNP)를 주입하기 전후에 PET-MRI 이미지를 획득하고 평가하였다. 획득한 각 영상에 대해 관심영역(ROI)을 설정한 후, 분할하여 병변의 면적을 계산하였을 때 PET 영상이 MRI 영상보다 더 크고 정확했다. 특히 동시 PET-MRI 영상은 주변 연조직과 함께 정확한 병변을 묘사하였다. 평균 및 표준편차 값은 조영제 주입 여부에 관계없이 PET 영상 또는 PET-MRI 동시 영상보다 MRI 단독 영상에서 더 높게 나타났다. 또한 동시 PET-MRI 영상 값이 PET 영상보다 평균 및 표준편차 값이 높게 나타났다. ¹⁸F-FDG 라벨링된 MNP 조영제와 동시 PET-MRI 영상을 표적 영상으로 사용하고 ¹⁸F-FDG 조영제만을 원본 이미지로 사용했을 때의 피크 신호 대 잡음비(PSNR) 값은 모든 실험에서 유의미 하게 나타났다. 결론적으로 동시 PET-MRI 영상에서 결합된 ¹⁸F-FDG 표지 MNP 조영제가 유용함을 확인하였다. 다양한 핵종을 사용할 수 있는 SPECT-MRI 영상 연구를 통해 진단과 치료를 동시에 할 수 있는 제제를 개발하기 위해서는 향후 연구가 필요할 것이다.

중심단어: 동시PET-MRI, 조영제, 조영효과 평가, 영상처리, 최대신호대잡음비(PSNR)

연구자 정보 이력

	성명	소속	직위
(제1저자)	이길재	충북대학교 대학원 의용생체공학과	박사과정
(공동저자)	이훈재	연세대학교세브란스병원-한국생명공학연구소 병설 의료융합연구소	연구교수
(교신저자)	이태수	충북대학교 대학원 의용생체공학과	교수